Journal of the European Ceramic Society xxx (xxxx) xxx–xxx

Contents lists available at ScienceDirect

Journal of the European Ceramic Society

journal homepage: www.elsevier.com/locate/jeurceramsoc

Original Article

Structure characterization and microwave dielectric properties of $LiGa_5O_8$ ceramic with low-ε_r and low loss

Laiyuan Ao[a,c], Ying Tang[a,b,*], Jie Li[a,*], Weishuang Fang[a], Lian Duan[a], Congxue Su[a], Yihua Sun[c], Laijun Liu[a], Liang Fang[a,c,*]

[a] Guangxi Key Laboratory of Optical and Electronic Materials and Devices, College of Material Science and Engineering, Guilin University of Technology, Guilin, 541004, China
[b] Key Laboratory of Nonferrous Materials and New Processing Technology, Ministry of Education, Guilin University of Technology, Guilin 541004, China
[c] College of Materials and Chemical Engineering, Key Laboratory of Inorganic Nonmetallic Crystalline and Energy Conversion Materials, China Three Gorges University, Yichang, 443002, China

ARTICLE INFO

Keywords:
Inverse spinel structure
$LiGa_5O_8$
Microwave dielectric properties

ABSTRACT

$LiGa_5O_8$ ceramics with inverse spinel structure were prepared in a temperature range of 1200–1300 °C by solid-state reaction method. $LiGa_5O_8$ ceramics crystallized in cubic structure with space group $P4_332$, in which Li^+ and Ga^{3+} distributed in the octahedral B sites with 1:3 ordering. The optimal microwave dielectric properties with ε_r = 10.51, $Q \times f$ = 127,040 GHz, and τ_f = –60.16 ppm/°C were achieved at 1260 °C for 6 h. Microwave dielectric properties were discussed in combination with the intrinsic characteristics of crystal structure by packing fraction, Raman spectra, and infrared reflectivity spectrum. Additionally, $CaTiO_3$ was used to suppress τ_f of $LiGa_5O_8$ ceramics to near zero, and optimized performances of ε_r = 12.79, $Q \times f$ = 109,752 GHz and τ_f = +4.07 ppm/°C were obtained for $0.94LiGa_5O_8$-$0.06CaTiO_3$ ceramics at 1260 °C. These bright spots make $LiGa_5O_8$ ceramic a potential candidate for 5 G and millimeter wave technology.

1. Introduction

Recently, microwave dielectric ceramics (MWDCs) are widely utilized in the Internet of things, mobile communications, GPS, and ultra-high-speed LAN due to lightweight, compact bulk, and outstanding dielectric performances [1–3]. With the development of 5 G communications technology to millimeter wave band, the working frequency of 24–30 GHz, or 60–70 GHz, the delay time of signal transmission (less than 1 ms) has been greatly reduced [4,5]. Therefore, it stimulates the development of microwave dielectric ceramics towards low dielectric constant (ε_r), high quality factor ($Q \times f$), and near-zero temperature coefficient of resonance frequency (τ_f) [6–8].

Spinel-structured ceramics with the formula AB_2O_4 have been received widespread attention due to their outstanding physicochemical properties. Generally speaking, spinel-structured materials can be divided into normal spinel, partial spinel and inverse spinel according to the distributions of cations [9]. Many studies concluded that cation ordering distribution plays an important role in enhancing the $Q \times f$ value of microwave dielectric ceramics, such as $Ba(Zn_{1/3}Ta_{2/3})O_3$, $Ba(Mg_{1/3}Ta_{2/3})O_3$ and $Ba_4LiNb_3O_{12}$ [10–13]. Recently, a large number of Li-containing spinel-structured compounds with different cation ordering in the octahedral site (B-site) have been reported, which possessing outstanding microwave dielectric performances. Firstly, Sebastian et al. reported $Li_2ATi_3O_8$ (A = Zn, Mg, and Co) [14–16] and $Li_2AGe_3O_8$ (M = Zn, Co, and Ni) [17,18] spinel ceramics with the B-site 1:3 ordered. For example, the $Li_2AM_3O_8$ (A = Mg, Zn, Co, Ni; M = Ti, Ge) ceramics showed good microwave dielectric properties with ε_r = 8 ~ 29, $Q \times f$ = 40,500 ~72,000 GHz and τ_f = –78 ~ +3.2 ppm/°C. Besides, $LiZnNbO_4$ ceramics sintered at 950 °C with Li^+ and Nb^{5+} 1:1 orderly occupying the B-site had a microwave dielectric performance of ε_r = 14.6, $Q \times f$ = 47,200 GHz and τ_f = −64.5 ppm/°C [19]. Recently, $LiAl_5O_8$ ceramics reported by Lan et al. also showed cations 1:3 ordered distribution at the B site, with the microwave dielectric properties of ε_r = 8.43, $Q \times f$ = 49,300 GHz, and τ_f = –38 ppm/°C at 1600 °C [20].

Considering the similar crystal structure and lower synthesis temperature compared with $LiAl_5O_8$, $LiGa_5O_8$ has attracted our attention. $LiGa_5O_8$ had an inverse spinel structure and underwent the first-order transition caused by the 1:3 ordering of Li^+ and Ga^{3+} at the octahedral site at 1140 °C with decreasing temperature [21]. The ordered $LiGa_5O_8$ can be written as $(Ga_2)^A(LiGa_3)^BO_8$, in which Li^+ and partial Ga^{3+}

* Corresponding authors at: Guangxi Key Laboratory of Optical and Electronic Materials and Devices, College of Material Science and Engineering, Guilin University of Technology, Guilin, 541004, China.
E-mail addresses: tangyinggl001@aliyun.com (Y. Tang), jielee2019@aliyun.com (J. Li), fanglianggl001@aliyun.com (L. Fang).

https://doi.org/10.1016/j.jeurceramsoc.2020.06.017
Received 22 February 2020; Received in revised form 1 June 2020; Accepted 6 June 2020

occupy the octahedral (B site) in a 1:3 long-range order and the remainder of the Ga^{3+} ions are tetrahedrally coordinated (A site) [22]. The vibrational spectra and photoluminescence of $LiGa_5O_8$ have been reported [23,24]. Besides, $LiGa_5O_8$: (Ni^{2+}, Mn, Co, and Cr^{3+}) [25–28] were successfully prepared through various routes, and their optical properties were studied. In this work, we prepared $LiGa_5O_8$ ceramics via a traditional solid-state reaction method, and focused on the sintering behavior, crystal structure, infrared reflectivity spectrum, and the relationship between Raman spectra and their microwave dielectric properties.

2. Experimental

$LiGa_5O_8$ ceramics were fabricated by the solid-state method with high purity Li_2CO_3 (> 99.99 %) and Ga_2O_3(> 99.99 %) as raw materials were weighted following stoichiometry. And then milled for 4 h with ZrO_2 balls and ethanol as media, then the resultant slurry was dried and calcined at 1000 ℃ for 6 h. Re-milled for 6 h and dried, the dried powders mixed with 5 wt.% PVA and pressed into cylindrical pellets (6.5 mm in height and 10 mm in diameter). To suppress the evaporation of lithium, all samples were placed in a small crucible, the same component powders were filled in the crucible, which was covered with an alumina crucible. Then the samples were sintered at 1200–1300 ℃ for 6 h in air with a heating rate of 5 ℃/min, and cooled to room temperature with the furnace.

The apparent density of samples was measured by the Archimedes method, the crystalline phase was analyzed by powder X-ray diffractometer (XRD) on a Panalytical X'Pert PRO diffractometer with Cu $K\alpha_1$ radiation. Lattice parameters were calculated with Rietveld refinement using Fullprof software accomplished based on XRD data. A Raman spectrometer (Thermo Fisher Scientific DXR, USA) was used to measure the room temperature Raman spectrum with a spectral line of 532 nm and a range of 100-1000 cm^{-1}. The polished ceramic samples were thermally etched at a temperature of 80 ℃ below the sintering temperature for 30 min, scanning electron microscopes (FESEM; S4800, Hitachi, Tokyo, Japan) and energy dispersive spectrometer (EDS) were used to conduct microstructure analysis. JEOL JEM-2100 F TEM was used to collect high-resolution transmission electron microscope (HRTEM) and selected area electron diffraction (SAED) patterns at a working voltage of 200 kV. Room-temperature infrared reflectivity spectroscopy was recorded using the Bruker IFS 66v FT-IR in the infrared beamline station (U4) of the National Synchrotron Radiation Laboratory (NSRL), China. ε_r and $Q \times f$ values of the fired ceramics were measured using Agilent N5230A network analyzer, and τ_f values were obtained using a temperature chamber (Delta 9039, Delta Design, San Diego, CA) and calculated as follows:

$$\tau_f = \frac{f_{85} - f_{25}}{f_{25} \times (85 - 25)} \quad (1)$$

where, f_{85} and f_{25} were the resonant frequency at 85 ℃ and 25 ℃, reflectivity.

3. Results and discussion

The XRD patterns of $LiGa_5O_8$ ceramics sintered at 1200–1300 ℃ for 6 h are presented in Fig. 1. All the diffraction peaks matched well with JCPDS card No.00-038-1371 of $LiGa_5O_8$, and no secondary phase was detected. All the XRD patterns show low angle superlattice reflections, which can be indexed based on a primitive cubic lattice, having the Miller indices 110, 210, and 211. Hence, the ordered cubic-structural phase with the space group $P4_332$ was formed.

Rietveld refinement patterns of $LiGa_5O_8$ ceramics sintered at 1260 ℃ are shown in Fig. 2(a). The refined cell parameters were $a = b = c = 8.2040$ Å, $\alpha = \beta = \gamma = 90^\circ$ and $V = 552.1752(7)$ $Å^3$, with acceptable reliability factors of the profile $R_p = 6.27$ %, $R_{wp} = 9.06$ % and

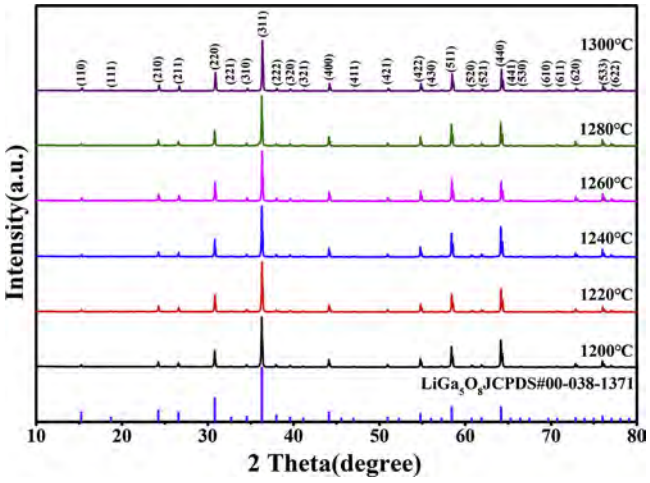

Fig. 1. Room-temperature XRD patterns of $LiGa_5O_8$ ceramics sintered at different temperatures.

$R_{exp} = 2.50$ %. The refined atomic coordinate parameters of $LiGa_5O_8$ ceramics are listed in Table S1 (Supplementary information). A schematic structure of $LiGa_5O_8$ is illustrated in Fig. 2(b). Li^+ and $Ga(1)^{3+}$ cations orderly occupy the B site, the $Ga(2)^{3+}$ cations randomly occupy the A site, and the $Ga(1)^{3+}$ cations at the B site are adjacent to four Ga (1) and two Li cations. Adjacent octahedral edges are shared, and tetrahedrons are corner-linked with adjacent three octahedrons. HRTEM and SAED were used to further study the ordered structure of the $LiGa_5O_8$ ceramics. The SAED pattern consists of sharp diffraction spots, indicating that the $LiGaO_5$ grains have good crystallinity, and superlattice reflection is clearly shown indicating that high-order Li^+ (4a) and Ga^{3+} (12d) are distributed in the octahedral sites (Fig. 2(c)). The HRTEM image recorded along the [1, -1, -1] zone axes shows the (1 1 0) and (2 2 1) plane with a spacing distance of 0.5887 nm and 0.3394 nm in consistent with the SAED and XRD results (Fig. 2(d)). It is further verified that $LiGa_5O_8$ prepared in this experiment belongs to the cubic inverse spinel structure with space group $P4_332$.

The SEM images of $LiGa_5O_8$ ceramics sintered at different temperatures for 6 h are shown in Fig. 3(a–c). Obviously, as the sintering temperature increased, the grains grew rapidly and the pores disappeared. As the temperature rose to 1260 ℃, a dense and uniform microstructure was obtained, and the grain boundaries were clearly visible, which helpe reduce microwave dielectric loss. However, as the temperature further increased, the grain boundary movement rate increased, resulting in the grain boundary moving faster than the pores, the grains grew abnormally finally causing the deterioration of microwave dielectric performances (Fig. 3(c)).

Fig. 4(a) shows the variation in bulk density and relative density of $LiGa_5O_8$ ceramics with sintering temperature. Increasing the sintering temperature led to a rapid increase in bulk density and relative density, which reached the maximum values of 5.669 g/cm^3 and 97 % at 1260 ℃, respectively, and slightly decreased thereafter. The $LiGa_5O_8$ ceramic sintered at 1260 ℃ possessed optimum properties with a low ε_r of 10.51, high $Q \times f$ value of 127,040 GHz and relatively large negative τ_f of −60.16 ppm/℃ (Fig. 4(b)–(d)). Generally, the second phase, relative density, and ionic polarizability are the main influence factors of permittivity of ceramic materials [29]. In this work, the effect of the second phase on dielectric constant can be ignored. Besides, the theoretical permittivity of $LiGa_5O_8$ ceramic can be calculated by the Clausius–Mossotti equation [30]:

$$\varepsilon_{th} = \frac{3V + 8\pi\alpha}{3V - 4\pi\alpha} \quad (2)$$

where V refers to the cell volume, α is molecular polarizability. According to the Shannon's additive rule $\alpha(LiGa_5O_8) = \alpha(Li^+) +$

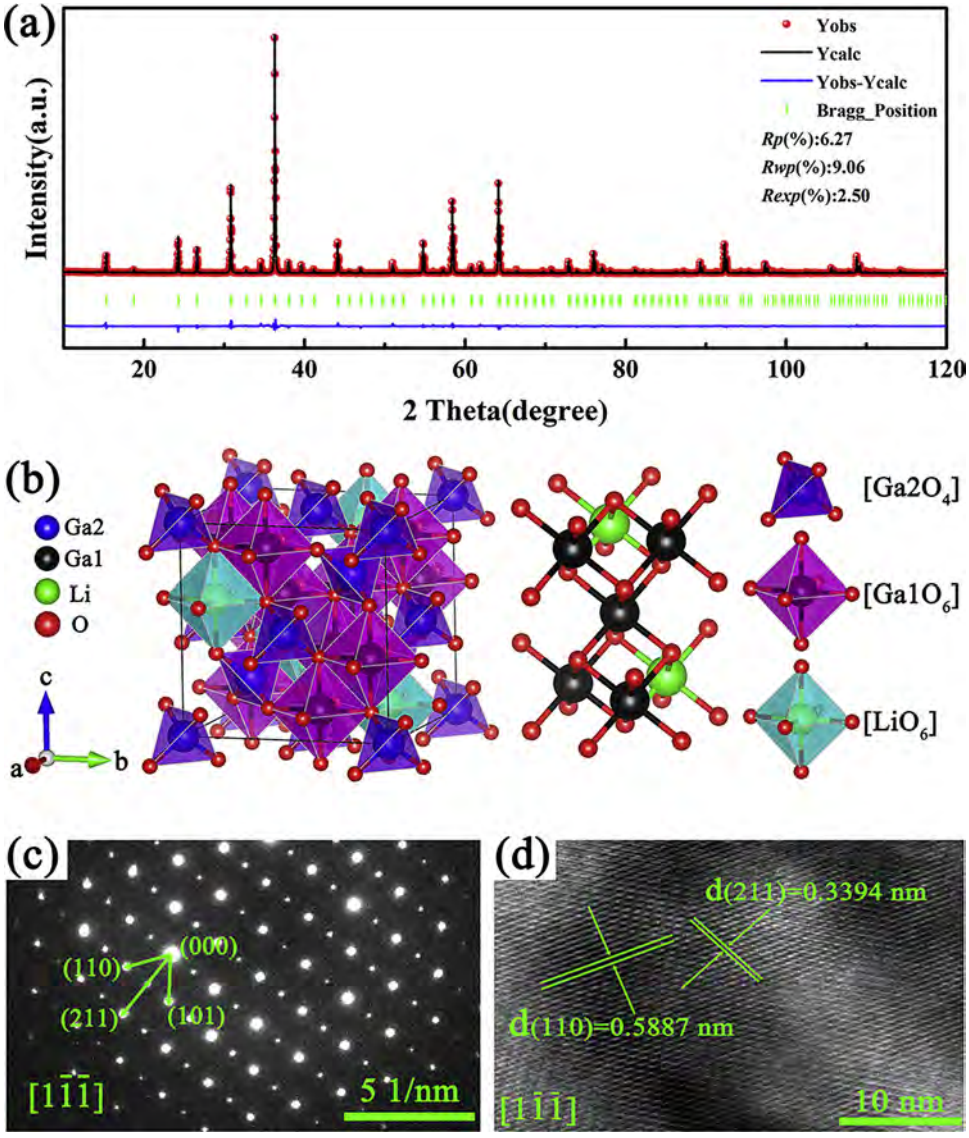

Fig. 2. (a) The Rietveld refined patterns, (b) crystal structure, (c) SAED image and (d) HRTEM of $LiGa_5O_8$ ceramic powders sintered at 1260 ℃ for 6 h.

$5\alpha(Ga^{3+}) + 8\alpha(O^{2-})$; $\alpha(Li^{+})$, $\alpha(Ga^{3+})$ and $\alpha(O^{2-})$ were the ions polarizabilities [31]. The theoretical permittivity of $LiGa_5O_8$ was 10.09, deviating from the measured value of 3.57%–11.61%. The ε_r was corrected by $\varepsilon_{corrected} = \varepsilon r(1 + 1.5P)$, P referring to fractional porosity, the $\varepsilon_{corrected}$ values were higher than the measured values (Fig. 4(b)).

The quality factor is affected by two factors, intrinsic (e.g. lattice vibration and ionic polarization) and extrinsic (such as grain boundaries, defects, impurities and their order and disorder) [32,33]. As can be seen from Fig. 4(c), as the sintering temperature increases, $Q \times f$ gradually increases, then reaches a maximum value of ~127,040 GHz at 1260 ℃, which is related to densification and uniform microstructure. Upon further increasing the temperature, the $Q \times f$ gradually descends to 109,716 GHz, due to the microstructure degradation caused by the abnormal grain growth. According to the report of Kim et al. [34], $Q \times f$ is closely related to the packing fraction, which is defined as follows:

$$\text{Packing fraction}(P_f) = \frac{\text{volume of packed ions}}{\text{volume of unie cell}} \times 4 \times 100\% \quad (3)$$

the positive correlation between P_f and $Q \times f$ is also shown in Fig. 4(c).

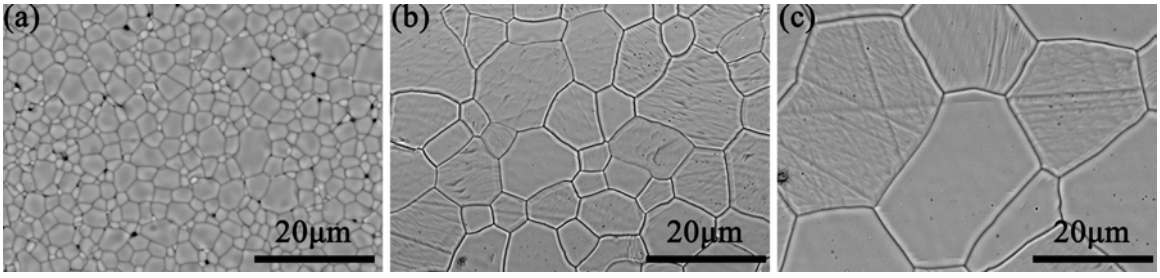

Fig. 3. $LiGa_5O_8$ ceramics sintered at (a)1220 ℃, (b)1260 ℃, (c)1300 ℃.

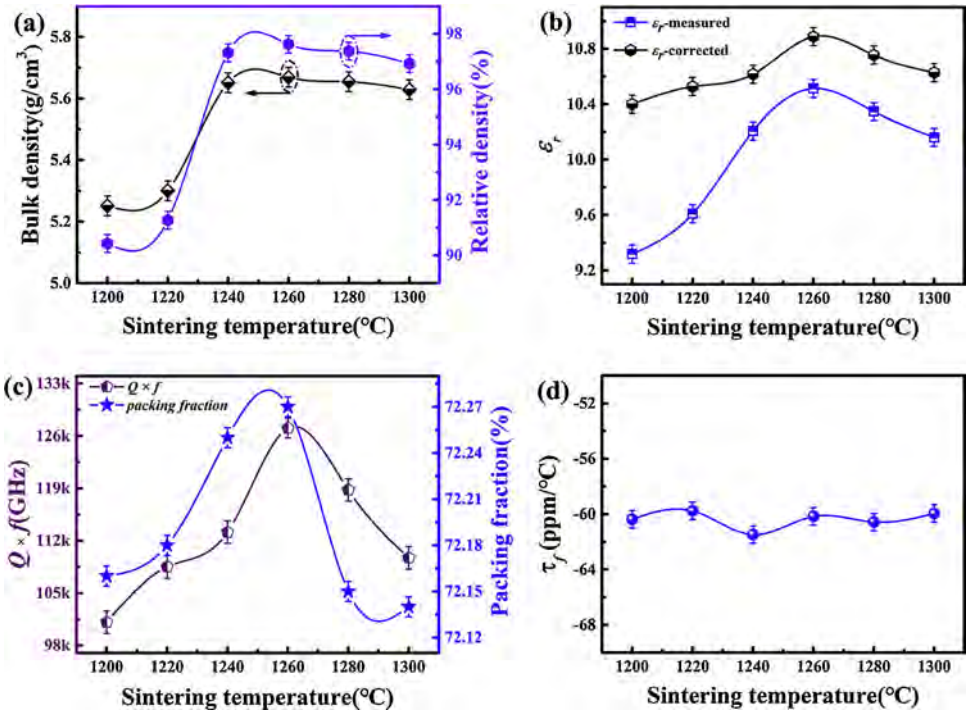

Fig. 4. (a) Relative densities and bulk density, (b) dielectric constant, (c) packing fraction and $Q \times f$, (d) τ_f values of the $LiGa_5O_8$ ceramics sintered at various temperatures.

Increasing P_f will reduce the lattice vibration and thus enhance the $Q \times f$ value [35], the maximum calculated P_f of $LiGa_5O_8$ ceramic is 72.27 % sintered at 1260 ℃ for 6 h.

Raman spectrum is an effective tool to research the lattice vibration information, whose variation will cause changes in Raman shift and Raman fullwidth at half maximum (FWHM) [36]. Fig. S1 illustrates the Raman spectra of $LiGa_5O_8$ samples sintered at 1200–1300 ℃. In $LiGa_5O_8$ ceramics, the Raman mode around 424 cm^{-1} corresponds to the tensile vibration of the Ga-O bond and vibration of the [GaO_6] octahedra, which affects the inherent dielectric characteristics of the ceramics [17]. Fig. 5(a) shows the alteration of the permittivity and Raman shift of 424 cm^{-1} mode with the sintering temperature. The various trend in dielectric constant is opposite to the change in Raman shift, this is because the [GaO6] octahedra corresponding to the 424 cm^{-1} mode at a higher wavenumber has higher vibration energy as the temperature increases, resulting in a lower dielectric constant. Similarly, the FWHM is inverse relation to the variation in $Q \times f$ (Fig. 5(b)), ascribing to the weakening of the damping behavior of 424 cm^{-1} mode as its FWHM lowered, resulting in the decrease of intrinsic dielectric loss [16].

Far-infrared reflectance spectroscopy was used to further study the intrinsic dielectric response of $LiGa_5O_8$ ceramic, which analyzed by the harmonic oscillator model (the Lorentz three-parameter classical model) as follows:

$$\varepsilon^*(\omega) = \varepsilon_\infty + \sum_{j=1}^{n} \frac{\omega_{pj}^2}{\omega_{oj}^2 - \omega^2 - j\gamma_j\omega} \tag{4}$$

where $\varepsilon^*(\omega)$ is a complex dielectric function, ε_∞ represents the permittivity caused by the electronic polarization at high frequencies, γj, ω_{oj}, and ω_{pj} are the damping factor, the transverse frequency, and plasma frequency of the j-th Lorentz oscillator, respectively, and n is the number of transverse phonon modes. Relationship between complex reflectivity $R(\omega)$ and permittivity can be expressed as:

$$R(\omega) = \left| \frac{1 - \sqrt{\varepsilon^*(\omega)}}{1 + \sqrt{\varepsilon^*(\omega)}} \right|^2 \tag{5}$$

Assuming that within the microwave region $\omega << \omega_{oj}$, the real part and imaginary part of microwave permittivity can be written as:

$$\varepsilon'(\omega) = \varepsilon_\infty + \sum_{j=1}^{n} \Delta\varepsilon_j' = \varepsilon_\infty + \sum_{j=1}^{n} \frac{\omega_{pj}^2}{\omega_{oj}^2} \tag{6}$$

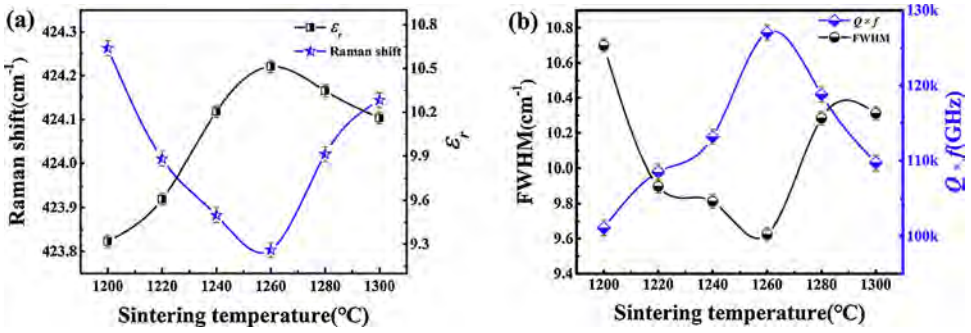

Fig. 5. (a) The variation of the dielectric constant and Raman shift at 424 cm^{-1} (b) $Q \times f$ value and Raman fullwidth at half maximum (FWHM) at 424 cm^{-1} as a function of sintering temperature.

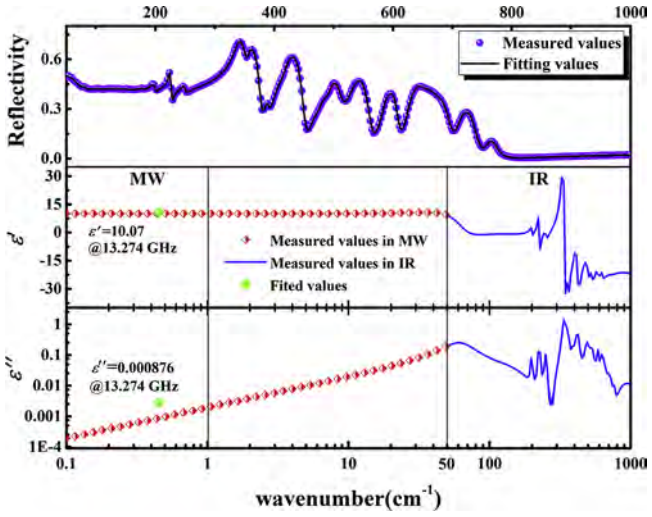

Fig. 6. Measured and fitted infrared reflectivity spectra and the real and imaginary parts of the complex dielectric response of $LiGa_5O_8$ ceramics.

$$\tan\delta = \frac{\varepsilon''}{\varepsilon'} = \omega \sum_{j=1}^{n} \frac{\Delta\varepsilon_j \gamma_j}{\omega_{oj}^2(\varepsilon_\infty + \sum_{j=1}^{n}\Delta\varepsilon_j)} \quad (7)$$

The fitted IR reflectivity values and complex permittivity of $LiGa_5O_8$ ceramic are shown in Fig. 6. Table S2 lists the phonon parameters obtained from the fitting of the infrared reflectivity spectra of $LiGa_5O_8$ ceramic using Reffit software. According to the fitting parameters, the dielectric constant at the optical frequency is 1.77, and the calculated value in the microwave frequency is 10.07, which is close to the measured value of 10.51 at 13.274 GHz. It is confirmed that the polarization at the microwave frequency is dominated by the absorption of phonons in the far-infrared region [37]. The calculated $Q \times f$ value is 152,590 GHz, larger than the measured value of 127,040 GHz, which indicates that extrinsic factors (defects, grain boundaries, and grain size, etc.) may contribute to the $Q \times f$.

Fig. 4(d) shows the relationship between τ_f and sintering temperature. The τ_f value fluctuates around -60 ppm/°C for ceramics sintered at 1200–1300 °C, with a weak dependence on sintering temperature. Unfortunately, the large τ_f hinders its practical application, especially in harsh condition with a wide temperature range. Therefore, to improve temperature stability, $CaTiO_3$ ceramics with positive τ_f values were used to adjust the τ_f of $LiGa_5O_8$ materials by forming composite ceramics. The XRD patterns, and backscattered electron image (BSE) of $0.94LiGa_5O_8$-$0.06CaTiO_3$ ceramic sintered at 1260 °C for 6 h are shown in Fig. 7. Only diffraction peaks of $LiGa_5O_8$ and $CaTiO_3$ (JCPDS No.01-076-2400) were detected in the XRD patterns. From the BSE diagram, the grains with two different gray scales are clearly visible, the darker grains referring to $CaTiO_3$ and the lighter ones belonging to $LiGa_5O_8$, indicating that there is no chemical reaction between the two ceramics. Table 1 lists the microwave dielectric properties of composite (1-x)$LiGa_5O_8$-$x$$CaTiO_3$ (x represents the volume fraction) ceramics. Temperature stable ceramics of $0.94LiGa_5O_8$-$0.06CaTiO_3$ with a near-zero τ_f = +4.07 ppm/°C were obtained. Table 2 summarizes the microwave dielectric properties of some B-sites ordering Li-based spinel-structured ceramics. In comparison, the $LiGa_5O_8$ and $0.94LiGa_5O_8$-$0.06CaTiO_3$ composition ceramic possess low ε_r for high-speed data propagation and high-quality factor, which is beneficial for high-frequency selectivity. Therefore, $LiGa_5O_8$ ceramics have promising application prospects in 5 G and millimeter wave communication technology.

4. Conclusions

In the present work, $LiGa_5O_8$ ceramics with inverse spinel structure were synthesized at 1200–1300 °C. Rietveld refinement and SAED both confirmed the phase purity and ordered structure of $LiGa_5O_8$ with the space group $P4_332$. At the optimum sintering temperature of 1260 °C, dense ceramics with homogenous microstructure were obtained, with optimal microwave dielectric properties of ε_r = 10.51, $Q \times f$ = 127,040 GHz and τ_f = -60.16 ppm/°C. The relationship between microwave dielectric properties and Raman mode at 424 cm^{-1} were explained in detail. Besides, the intrinsic permittivity of 10.07 and $Q \times f$ value of 152,590 GHz was extrapolated by the fitted infrared reflectivity spectra. The large negative τ_f values were successfully tuned to near aero by forming $0.94LiGa_5O_8$-$0.06CaTiO_3$ composite ceramics sintered at 1260 °C for 6 h with ε_r = 12.79, $Q \times f$ = 109,752 GHz and τ_f = +4.07 ppm/°C. The low loss, feasible preparation, and outstanding microwave dielectric properties propose that $LiGa_5O_8$ ceramics are promising candidates for 5 G applications.

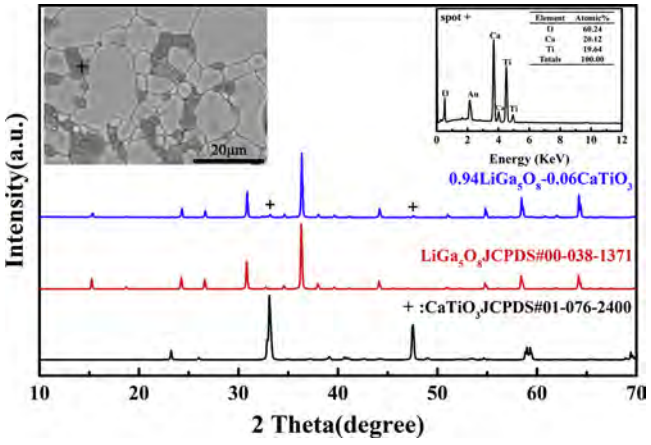

Fig. 7. The XRD patterns, Backscattered electron image (BSE), and EDS analysis of $0.94LiGa_5O_8$-$0.06CaTiO_3$ ceramics sintered at 1260 °C.

Table 1
Microwave dielectric properties of (1-x)$LiGa_5O_8$-$x$$CaTiO_3$ (x represents volume fraction) composite ceramics.

x value	S.T. (°C)	ε_r	$Q \times f$(GHz)	τ_f (ppm/°C)
0	1260	10.51 ± 0.1	127,040 ± 2000	−60.16 ± 2.1
0.04	1260	11.89 ± 0.1	115,822 ± 1800	−33.35 ± 1.5
0.06	1260	12.79 ± 0.1	109,752 ± 2000	+4.07 ± 1.1
0.07	1260	13.94 ± 0.1	98,280 ± 1900	+13.63 ± 1.2
0.08	1260	14.66 ± 0.1	87,697 ± 2100	+36.56 ± 1.1

Table 2
Microwave dielectric properties of B-sites ordering Li-based spinel ceramics.

ceramics	S.T. (°C)	ε_r	$Q \times f$(GHz)	τ_f(ppm/°C)	Reference
$Li_2ZnTi_3O_8$	1075	25.6	72,000	−11.2	[14]
$Li_2MgTi_3O_8$	1075	27.2	42,000	+3.2	[14]
$Li_2CoTi_3O_8$	1025	28.9	52,600	+7.4	[16]
$Li_2ZnGe_3O_8$	945	10.5	47,400	−63.9	[17]
$Li_2CoGe_3O_8$	950	9.0	40,500	−42	[18]
$Li_2NiGe_3O_8$	940	8.6	42,200	−78.2	[18]
$LiAl_5O_8$	1600	8.43	49,300	−38	[20]
$LiGa_5O_8$	1260	10.51	127,040	−60.16	This work
$LiZnNbO_4$	950	14.6	47,200	−64.5	[19]

Declaration of Competing Interest

The authors declare that they have no known competing financial interests or personal relationships that could have appeared to influence the work reported in this paper.

Acknowledgments

This work was financially supported by the Natural Science Foundation of China (Nos. 21761008and 21965009), the Natural Science Foundation of Guangxi Zhuang Autonomous Region (Nos. 2018GXNSFAA138175, and 2018GXNSFBA281093), the Project of Scientific Research and Technical Exploitation Program of the Guangxi Zhuang Autonomous Region (No. AA18118008, AA18118034 and AA18118023), and Projects of Education Department of Guangxi Zhuang Autonomous Region (No. 2018KY0255) and High level innovation team and outstanding scholar program of Guangxi Institutes. The author thanks the administrator of the IR beamline workstation at the National Synchrotron Radiation Laboratory (NSRL) for their assistance in IR measurements.

Appendix A. Supplementary data

Supplementary material related to this article can be found, in the online version, at doi:https://doi.org/10.1016/j.jeurceramsoc.2020.06.017.

References

[1] J.E.F.S. Rodrigues, P.J. Castro, P.S. Pizani, W.R. Correr, A.C. Hernandes, Structural ordering and dielectric properties of $Ba_3CaNb_2O_9$-based microwave ceramics, Ceram. Int. 42 (2016) 18087–18093.
[2] C.C. Xia, D.H. Jiang, G.H. Chen, Y. Luo, B. Li, C.L. Yuan, C.R. Zhou, Microwave dielectric ceramic of $LiZnPO_4$ for LTCC applications, J. Mater. Sci. Mater. Electron. 28 (2017) 1206–12031.
[3] B. Synkiewicz-Musialskaa, D. Szwagierczaka, J. Kulawika, N. Pałkab, P.R. Bajurko, Impact of additives and processing on microstructure and dielectric properties of willemite ceramics for LTCC terahertz applications, J. Eur. Ceram. Soc. 40 (2020) 362–370.
[4] Q.B. Lin, K.X. Song, B. Liu, H.B. Bafrooei, D. Zhou, W.T. Su, F. Shi, D.W. Wang, H.X. Lin, Ian M.Reaney, Vibrational spectroscopy and microwave dielectric properties of $AY_2Si_3O_{10}$(A = Sr, Ba) ceramics for 5G applications, Ceram. Int. 46 (2020) 1171–1177.
[5] G.H. Chen, J.S. Chen, X.L. Kang, Y. Luo, Q. Feng, C.L. Yuan, Y. Yang, T. Yang, Structural and microwave dielectric properties of new $CaTi_{1-x}(Al_{0.5}Nb_{0.5})_xO_3$ thermally stable ceramics, J. Alloys Compd. 675 (2016) 301–305.
[6] J.Q. Chen, Y. Tang, H.C. Xiang, L. Fang, H. Porwal, C.C. Li, Microwave dielectric properties and infrared reflectivity spectra analysis of two novel low-firing $AgCa_2B_2V_3O_{12}$ (B = Mg, Zn) ceramics with garnet structure, J. Eur. Ceram. Soc. 38 (2018) 4670–4676.
[7] Z.W. Zhang, L. Fang, H.C. Xiang, M.Y. Xu, Y. Tang, H. Jantunen, C.C. Li, Structural, infrared reflectivity spectra and microwave dielectric properties of the $Li_7Ti_3O_9F$ ceramic, Ceram. Int. 45 (2019) 10163–10169.
[8] S.H. Lei, H.Q. Fan, X.H. Ren, J.W. Fang, L.T. Ma, Z.Y. Liu, Novel sintering and band gap engineering of $ZnTiO_3$ ceramics with excellent microwave dielectric properties, J. Mater. Chem. C 5 (2017) 4040–4047.
[9] X.C. Lu, Z.H. Du, B. Quan, W.J. Bian, H.K. Zhu, Q.T. Zhang, Structural dependence of microwave dielectric properties of Cr^{3+}-substituted $ZnGa_2O_4$ spinel ceramics: crystal distortion and vibration modes study, J. Mater. Chem. C 7 (2019) 8261–8268.
[10] D.J. Barber, K.M. Moulding, Ji. Zhou, M.Q. Li, Structural order in Ba $(Zn_{1/3}Ta_{2/3})O_3$, $Ba(Zn_{1/3}Nb_{2/3})O_3$ and $Ba(Mg_{1/3}Ta_{2/3})O_3$ microwave dielectric ceramics, J. Mater. Sci. 32 (1997) 1531–1544.
[11] V. Tolmer, G. Desgardin, Low-temperature sintering and influence of the process on the dielectric properties of $Ba(Zn_{1/3}Ta_{2/3})O_3$, J. Am. Ceram. Soc. 80 (1997) 1981–1991.
[12] N. Ichinose, T. Shimada, Effect of grain size and secondary phase on microwave dielectric properties of $Ba(Mg_{1/3}Ta_{2/3})O_3$ and $Ba([Mg, Zn]_{1/3}Ta_{2/3})O_3$ systems, J. Eur. Ceram. Soc. 26 (2006) 1755–1759.
[13] L. Fang, C.C. Li, X.Y. Peng, C.Z. Hu, B.L. Wu, H.F. Zhou, $Ba_4LiNb_{3-x}Ta_xO_{12}$(x = 0–3): a series of High-Q microwave dielectrics from the twinned 8H hexagonal perovskites, J. Am. Ceram. Soc. 93 (2010) 1229–1231.
[14] S. George, M.T. Sebastian, Synthesis and microwave dielectric properties of novel temperature stable high Q, $Li_2ATi_3O_8$(A = Mg, Zn) ceramics, J. Am. Ceram. Soc. 93 (2010) 2164–2166.
[15] H.F. Zhou, X.L. Chen, L. Fang, D.J. Chu, H. Wang, A new low-loss microwave dielectric ceramic for low temperature cofired ceramic applications, J. Mater. Res. 25 (2010) 1235–1238.
[16] L. Fang, D.J. Chu, H.F. Zhou, X.L. Chen, Z. Yang, Microwave dielectric properties and low temperature sintering behavior of $Li_2CoTi_3O_8$ ceramic, J. Alloys Compd. 509 (2011) 1880–1884.
[17] H.C. Xiang, L. Fang, W.S. Fang, Y. Tang, C.C. Li, A novel low-firing microwave dielectric ceramic $Li_2ZnGe_3O_8$ with cubic spinel structure, J. Eur. Ceram. Soc. 37 (2017) 625–629.
[18] H. Luo, L. Fang, H.C. Xiang, Y. Tang, C.C. Li, Two novel low-firing germanates $Li_2MGe_3O_8$ (M = Ni, Co) microwave dielectric ceramics with spinel structure, Ceram. Int. 43 (2017) 1622–1627.
[19] L.X. Pang, D. Zhou, A low-firing microwave dielectric material in Li_2O–ZnO–Nb_2O_5 system, Mater. Lett. 64 (2010) 2413–2415.
[20] X.K. Lan, J. Li, J.P. Li, F. Wang, W.Z. Lu, X.C. Wang, W. Lei, Phase evolution and microwave dielectric properties of novel $LiAl_{5-x}Zn_xO_{8-0.5x}$-based ($0 \leq x \leq 0.5$) ceramics, J. Am. Ceram. Soc. 103 (2020) 1105–1112.
[21] K. Hara, Y. Ishibashi, Raman scattering study of lithium gallate $LiGa_5O_8$, J. Phys. Soc. Jpn. 55 (1986) 4500–4503.
[22] J. Ahman, G. Svensson, J. Albertsson, Structure of $LiGa_5O_8$, Acta Chem. Scand. 50 (1996) 391–394.
[23] V.G. Keramidas, B.A. Deangelis, W.B. White, Vibrational spectra of spinels with cation ordering on the octahedral sites, J. Solid State Chem. 15 (1975) 233–245.
[24] K.H. Park, H.L. Park, S. Mho, Compositional dependence of photoluminescence (PL) of $ZnGa_2O_4$: Li^+; Li^+ ion incorporated as $LiGa_5O_8$, $LiGaO_2$, and Li_2O, J. Lumin. 93 (2001) 205–212.
[25] J.F. Donegan, F.J. Bergin, T.J. Glynn, G.F. Imbusch, J.P. Remeika, The optical spectroscopy of $LiGa_5O_8$: Ni^{2+}, J. Lumin. 35 (1986) 57–63.
[26] T. Abritta, N.V. Vugman, F. de Souza Barros, N.T. Melamed, Optical properties of $LiGa_5O_8$: Mn, J. Lumin. 31&32 (1984) 281–283.
[27] J.F. Donegan, F.J. Bergin, G.F. Imbusch, J.P. Remeika, Luminescence from $LiGa_5O_8$: Co, J. Lumin. 31&32 (1984) 278–280.
[28] H. Szymczak, M. Wardzynska, I.E. Mylnikova, Optical spectrum of Cr^{3+} in the spinel $LiGa_5O_8$, J. Phys. C: Solid State Phys. 8 (1975) 3937–3943.
[29] D. Zhou, L.X. Pang, J. Guo, Z.M. Qi, T. Shao, Q.P. Wang, H.D. Xie, X. Yao, Clive A. Randall, Influence of Ce substitution for Bi in $BiVO_4$ and the impact on the phase evolution and microwave dielectric properties, Inorg. Chem. 53 (2014) 1048–1055.
[30] S.H. Yoon, D.W. Kim, S.Y. Cho, K.S. Hong, Investigation of the relations between structure and microwave dielectric properties of divalent metal tungstate compounds, J. Eur. Ceram. Soc. 26 (2006) 2051–2054.
[31] R.D. Shannon, Dielectric polarizabilities of ions in oxides and fluorides, J. Appl. Phys. 73 (1993) 348–366.
[32] M.R. Joung, J.S. Kim, M.E. Song, S. Nahm, Formation process and microwave dielectric properties of the $R_2V_2O_7$ (R = Ba, Sr, and Ca) ceramics, J. Am. Ceram. Soc. 92 (2009) 3092–3094.
[33] M.R. Joung, J.S. Kim, M.E. Song, S. Nahm, Formation and microwave dielectric properties of the $Mg_2V_2O_7$ ceramics, J. Am. Ceram. Soc. 92 (2009) 1621–1624.
[34] E.S. Kim, B.S. Chun, R. Freer, R.J. Cernik, Effects of packing fraction and bond valence on microwave dielectric properties of $A^{2+}B^{6+}O_4$(A^{2+}: Ca, Pb, Ba; B^{6+}: Mo, W) ceramics, J. Eur. Ceram. Soc. 30 (2010) 1731–1736.
[35] G.G. Yao, Synthesis and microwave dielectric properties of $Li_2ZnTi_3O_8$ ceramics by the reaction-sintering process, J. Ceram. Process. Res. 16 (2015) 41–44.
[36] L.X. Pang, D. Zhou, Z.M. Qi, W.G. Liu, Z.X. Yue, I.M. Reaney, Structure–property relationships of low sintering temperature scheelite-structured $(1-x)BiVO_4$-$xLaNbO_4$ microwave dielectric ceramics, J. Mater. Chem. C 5 (2017) 2695–2701.
[37] Y. Tang, M.Y. Xu, L. Duan, J.Q. Chen, C.C. Li, H.C. Xiang, L. Fang, Structure, microwave dielectric properties, and infrared reflectivity spectrum of olivine type Ca_2GeO_4 ceramic, J. Eur. Ceram. Soc. 39 (2019) 2354–2359.